

A Real-Time Vision System for Traffic Signs Recognition Invariant to Translation, Rotation and Scale

Bogusław Cyganek

AGH - University of Science and Technology
Al. Mickiewicza 30, 30-059 Kraków, Poland
cyganek@uci.agh.edu.pl

Abstract. In this paper a system is presented for real time recognition of the traffic signs. Sign detection is done by a method of adaptively growing window. Classification is based on matching of the modulo-shifted phase histograms. These are built from the stick component of the structural tensor rather than from an edge detector. To cope with inherent rotations of signs a novel measure is proposed for matching of the modulo-shifted histograms that also boosts responses of highly probable values. The method is tolerant of small translations, rotations and symmetrical changes of scale. It works also well under different lighting conditions and tolerates noise and small occlusions.

1 Introduction

Main goals of the Driver Assisting Systems (DAS) are to increase driving safety and comfort [7]. Automatic recognition of traffic signs (TSs) belongs to one of the major objectives of DAS. Much research has been done to develop real-time and accurate systems for this purpose. The works [8][11][15][4] and cited there references report advances in this area.

TSs are planar rigid objects of different shape and colour. These features are used in shape detectors [4][6]. However, images of signs can be diverted from the fronto-parallel view due to the inherent tilt and rotation, projective transformation of the camera system. They can be also affected by noise, dirt, weather and other factors. From these rotations are very cumbersome in classification of the circular signs, since our detectors cannot account for rotations of circular shapes. The proposed method can cope with this and other deformations. It is also able to classify all types of TSs.

The novelty of this paper comes from the fact of using the precise structural tensor (ST) for both, finding of image areas with sufficient structure and then computation of the phase of local orientations. Thanks to the matched filters, these parameters are obtained with sufficient accuracy. Classification is done by matching of the modulo shifted phase histograms. This allows detection and computation of the internal rotations of signs. Thanks to these features, the proposed method of TSs recognition is invariant to translation, rotation, proportional change of scale, as well as to the different lighting conditions (day and night) and small occlusions. Additionally, the method is fairly accurate and works in real time, i.e. it allows analysis of about ten or more frames per second which is sufficient for real applications.

2 Architecture of the Traffic Signs Recognition System

The proposed system, presented in Fig. 1, consists of two main modules: a detector of characteristic shapes and a sign classifier. In this paper we focus mostly on the latter.

TSs are *detected* solely based on their colour distributions. This is possible mostly due to the very pronounced colours of TSs and allows fast execution at the same time. Shape could be also used, however this requires additional computation time. A developed detector for triangular, rectangular and diamond shapes is presented in [6]. These, however, can be registered, so the internal rotation is cancelled. In consequence a classifier operating on a group of deformable prototypes is feasible [4]. However a real challenge are circular signs for which the internal rotation cannot be amended by the detector.

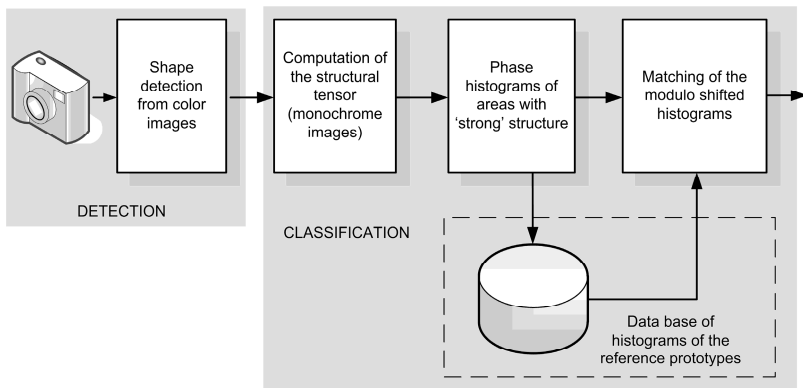


Fig. 1. The system consists of two modules: shape detection and sign classification

The main idea of detection of the circular TSs is to expand a rectangular window W in all eight direction around a place with high probability of existence of an object (see Fig. 2). Moreover, we do not assume that the tracked signal follows assumptions of the probability field. The only requirement is that the tracked region is described by a nonnegative “mass” function μ for which it is assumed that the higher its value, the strongest belief that a pixel belongs to an object. Thus, μ follows rather rules of a fuzzy membership function, although it can be a probability field as well. Hence, the versatility of the method.

Expansion in a given direction is possible iff there is a nonnegative increase in density of a new region. This is computed as a ratio of an object “mass” function divided by a number of pixels in a growing pane. In effect, starting from an initial size W_0 a final window W_F is reached which encompasses tightly an object. In practice it is sufficient to set a minimal thresholds on a “mass” update in all direction of expansion to avoid divisions. That is, a stop criteria in a direction k is expressed as follows:

$$\Delta\mu_k < \tau_k . \quad (1)$$

where τ_k denotes an expansion threshold. In our experiments, in which μ was a fuzzy membership function conveying degree of a match of colour, τ_k is in order of 0.1-10.

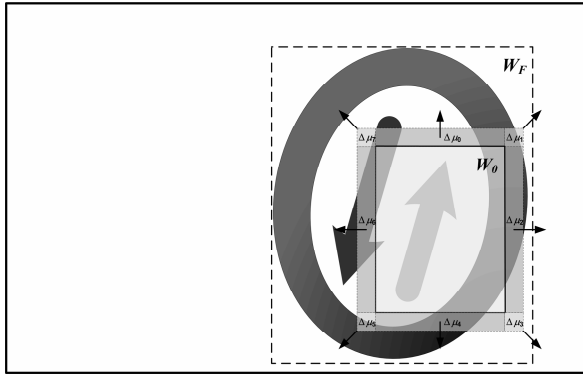


Fig. 2. Region growing technique for fast shape detection – an initial window grows in all eight directions until a stopping criteria are reached

The algorithm is guaranteed to stop either when condition (1) is fulfilled for all k , i.e. in all directions, or when borders of an image are reached. For more details see [4].

The first stage of the classification module in Fig. 1 is responsible for computation of the local orientations. The idea behind local orientations is to associate an orientation vector to each ‘sufficiently’ small region in an image, called a local neighbourhood of pixels. The orientation vectors are computed by means of the structural tensor [1][2]. Components of this tensor provide information on local phase, magnitude, and coherence values characteristic to the associated region [12]. Based on this, the phase histograms are created for each reference and test patterns. The idea of the orientation histograms for pattern matching was already proposed by many authors [13][10]. However, in our work we propose to use a precise structural tensor and compute phase histograms from structural places which correspond to the *stick component* of the structural tensor – presented in the next section (3). The histograms of the reference patterns are stored in a data base (DB). Then, classification is done by matching an input pattern with the data base. The matching is done with different measures and on modulo-shifted histograms, as presented in the section (4). In consequence the inherent rotation of an input pattern can be detected and measured.

The classification process is done *solely* in the monochrome representation of a detected sign, although local orientations can be easily computed from colour representations as well. However, this entails additional computation time with no significant improvement to the classification.

3 Phase Histograms from the Structural Tensor

Classification based on the orientation histograms has been proposed for recognition of different shapes [13][10]. We also follow this strategy, however with many modifications. The first one relies on a precise computation of the tensor components.

The idea behind the structural tensor is to describe each local neighbourhood LN of pixels with a single and dominating orientation, denoted by a vector \mathbf{w} in Fig. 3a.



Fig. 3. The idea behind the structural tensor is to represent a local neighbourhood LN with a single orientation vector \mathbf{w} , which is accurate if most of the gradients in LN coincide with \mathbf{w} (a). This can be checked by minimizing a cumulative sum of the residual vectors \mathbf{s} in LN (b).

Finding such \mathbf{w} is possible if the LN shows some regularity of its intensity signal. This can be measured by gradient vectors, computed for each point of the LN. If the gradient vectors are more less oriented in the direction of \mathbf{w} , then we can say that \mathbf{w} represents well the given LN. A fit measure can be defined as an average of the squared modules of vectors \mathbf{s} which are perpendicular projections of the gradients \mathbf{g} , onto the sought orientation vector \mathbf{w} . From Fig. 3b we find that

$$\mathbf{s} = \mathbf{g} - \mathbf{r} = \mathbf{g} - \mathbf{w} \frac{\|\mathbf{r}\|}{\|\mathbf{w}\|}. \tag{2}$$

Based on the above, the error function can be defined as follows [2]:

$$e(\mathbf{x}, \mathbf{x}_0) = \|\mathbf{s}\| = \left\| \mathbf{g}(\mathbf{x}) - \mathbf{w}(\mathbf{x}_0) \mathbf{g}^T(\mathbf{x}) \mathbf{w}(\mathbf{x}_0) \right\|, \text{ where } \mathbf{w}^T \mathbf{w} = 1. \tag{3}$$

The total error E is obtained integrating the square of $e(\mathbf{x}, \mathbf{x}_0)$ over all possible locations \mathbf{x} in the neighbourhood LN, using a Gaussian soft averaging filter G_σ :

$$E(\mathbf{x}_0) = \int_{\text{LN}} e^2(\mathbf{x}, \mathbf{x}_0) G_\sigma(\mathbf{x}, \mathbf{x}_0) d\mathbf{x}. \tag{4}$$

G_σ can be substituted for a robust function [2] which results in filtering *dependant* on a local structure. This makes the orientation vector \mathbf{w} well adapted to each local structure. However, a solution to this problem is iterative which appears to be too slow for our purposes. Continuing, by inserting (3) to (4) and expanding we obtain

$$E = - \int_{\text{LN}} \mathbf{g}^T \mathbf{g} G_\sigma(\mathbf{x}, \mathbf{x}_0) d\mathbf{x} + \mathbf{w}^T \left(\int_{\text{LN}} \mathbf{g}^T \mathbf{g} G_\sigma(\mathbf{x}, \mathbf{x}_0) d\mathbf{x} \right) \mathbf{w}, \tag{5}$$

Now, to find \mathbf{w} we have to solve the following optimization problem

$$\min_{\mathbf{w}} \|E\|, \tag{6}$$

subject to the constraint $\mathbf{w}^T \mathbf{w} = 1$. Substituting (5) into (6) we obtain

$$\min_{\mathbf{w}} \|E\| = \min_{\mathbf{w}} \left\| \int_{\text{LN}} \mathbf{g}^T \mathbf{g} G_\sigma(\mathbf{x}, \mathbf{x}_0) d\mathbf{x} - \mathbf{w}^T \left(\int_{\text{LN}} \mathbf{g}^T \mathbf{g} G_\sigma(\mathbf{x}, \mathbf{x}_0) d\mathbf{x} \right) \mathbf{w} \right\|. \tag{7}$$

Since $\mathbf{g}^T \mathbf{g} \geq 0$, then solution to (7) is equivalent to

$$\min_{\mathbf{w}} \|\mathbf{E}\| = \max_{\mathbf{w}} \left\{ \mathbf{w}^T \left(\int_{LN} \mathbf{g}^T \mathbf{g} G_{\sigma}(\mathbf{x}, \mathbf{x}_0) d\mathbf{x} \right) \mathbf{w} \right\} \Big|_{\mathbf{w}^T \mathbf{w} = 1}, \tag{8}$$

where the expression

$$\mathbf{T} = \int_{LN} \mathbf{g}^T \mathbf{g} G_{\sigma}(\mathbf{x}, \mathbf{x}_0) d\mathbf{x} \tag{9}$$

is the structural tensor. Using the method of Lagrange multipliers we find that the best orientation \mathbf{w} is an eigenvector of \mathbf{T} corresponding to its largest eigenvalue. This way, after simple computations, we obtain \mathbf{w} , as follows [12]:

$$\mathbf{w} = [T_{11} - T_{22} \quad 2T_{12}]^T, \tag{10}$$

where T_{ij} are components of \mathbf{T} . Finally, phase φ of a local structure represented by \mathbf{w} is given by the following formula:

$$\varphi(\mathbf{w}) = ATAN2(2T_{12}, T_{11} - T_{22}), \tag{11}$$

where $ATAN2$ is an arcus-tangent function of a quotient of its two arguments, which is also defined when its second argument approaches zero (result is $\pm\pi/2$ based on a sign of the first argument). Values of phase φ are taken to the phase histograms. The last question is in what places of an image φ should be actually computed.

As alluded to previously, a dominating orientation vector is well justified for image areas with ‘strong’ regularity. Computation of orientation histograms in edge points was already proposed by Freeman [10]. However, for relatively small objects, such as are pictograms of the TSSs, these do not provide sufficient support for reliable matching of their histograms. Therefore we propose to extend the structural places to the ones defined by so called *stick tensor components* which represent linear component of the structural tensor. The tensor \mathbf{T} is positive definite and therefore it can be decomposed as follows [14]:

$$\mathbf{T} = (\lambda_1 - \lambda_2) \underbrace{\bar{\mathbf{w}}_1 \bar{\mathbf{w}}_1^T}_{\mathbf{S}} + \lambda_2 \underbrace{(\bar{\mathbf{w}}_1 \bar{\mathbf{w}}_1^T + \bar{\mathbf{w}}_2 \bar{\mathbf{w}}_2^T)}_{\mathbf{B}}, \tag{12}$$

where \mathbf{S} and \mathbf{B} are the stick and the ball base tensors respectively, $\bar{\mathbf{w}}_1$ and $\bar{\mathbf{w}}_2$ are normalized eigenvectors, and $\lambda_{1,2}$ are real eigenvalues of \mathbf{T} for which $\lambda_1 \geq \lambda_2 \geq 0$. These can be computed from the following formula (λ_l takes ‘+’):

$$\lambda_{1,2} = \frac{1}{2} \left[(T_{11} + T_{22}) \pm \sqrt{(T_{11} - T_{22})^2 + 4T_{12}^2} \right]. \tag{13}$$

From the above formulas it is evident that areas that correspond only to the stick tensor component poses high value of λ_1 with small λ_2 at the same time. Therefore our criteria for areas of interest can be formulated as follows:

$$\frac{\lambda_2}{\lambda_1} \leq \kappa, \tag{14}$$

where κ is a threshold value, which in the experiments was less than 0.1. Inserting (13) into (14) we obtain

$$p \geq \frac{1 - \kappa}{1 + \kappa}, \tag{15}$$

where

$$p = \frac{\sqrt{(T_{11} - T_{22})^2 + 4T_{12}^2}}{T_{11} + T_{22}}, \text{ for } T_{11} + T_{22} \neq 0. \tag{16}$$

Thus, our algorithm for computation of the phase histograms in image areas with high stick-like structures is given as follows:

1. Set threshold κ (in practice ≤ 0.1) and initialize data structure for the histogram.
2. For each pixel position do
 3. Compute \mathbf{T} from discrete version of (9).
 4. Compute trace $m = T_{11} + T_{22}$.
 5. If $m > 0$ then
 6. Compute p from (16).
 7. If $p \geq (1 - \kappa) / (1 + \kappa)$ then
 8. Compute φ from (11) and add it to the histogram.

Let us observe that trace value m , computed in step 4 of the above algorithm, denotes an averaged squared magnitude of a signal gradient, since

$$m = \text{Tr}(\mathbf{T}) = T_{11} + T_{22} = \int_{\text{LN}} \nabla_x^2(I) d\mathbf{x} + \int_{\text{LN}} \nabla_y^2(I) d\mathbf{x} = \int_{\text{LN}} \|\nabla(I)\|^2 d\mathbf{x}. \tag{17}$$

Thus m can be thought of as a kind of an edge detector. However it is different than detectors proposed in [10] since m denotes an *averaged* gradient in a neighbourhood. Therefore it is more resistant to noise. In some applications, step 5 can be more restrictive to suppress noise. In such a case we replace 0 with a positive threshold.

Features are acquired only from the internal part of a detected sign, since we are interested in its pictogram. For this purpose a centre of a sign is found and the minimal perpendicular distance to the borders is assumed to be a starting radius. Then, the features are taken *only* from points which are distant no more than 70-85% of the found radius. This parameter is selected by a user. Thus, a circular region is cropped from the input image. This strategy is acceptable for all types of signs since recognition in a particular group of signs is based solely on their pictograms (Fig. 4).

Implementation of the ST is very simple and can be realized by a number of convolutions with different filter masks. However, very important is use of the precise directional filters for computation of the image derivatives. Their accuracy directly influences quality of the stored phases of LNs. In our realization the matched filters proposed by Farid *et al.* have shown sufficient precision for this purpose [9].

4 Recognition Based on the Phase Histograms

All information about the classified patterns comes in the form of binary phase histograms. Number of their bins $\#B$ is set by a user. Thus, the quantization factor is $360\% \#B$. To find the best prototype, a histogram \mathbf{b} of an input image is checked against all S reference histograms \mathbf{a}_s , which were precomputed and stored in the data base. However, since the signs can be rotated, we need to match all *modulo shifted* versions of the input histogram \mathbf{b} . Thus, our recognition process can be stated as the following minimization problem:

$$\arg \min_{\substack{1 \leq s \leq S \\ -\Delta r \leq r \leq +\Delta r}} D_{(\cdot)}(\mathbf{a}_s, \mathbf{b} \% r), \tag{18}$$

where $D_{(\cdot)}$ is a match measure, $\mathbf{b} \% r$ is an r -modulo shift of a histogram, r is in $\pm \Delta r$.

When thinking of histogram matching we can go two ways depending on how we treat these structures. If we look at histograms simply as vectors of data, we can apply any method of vector matching. However, the more appropriate is the probabilistic approach. In this case, we can treat each entry of the histogram as a discrete value of a probabilistic density function. Thus, matching two histograms is equivalent to matching two probabilistic densities [16].



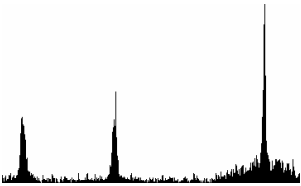


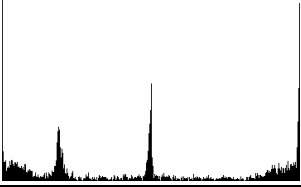


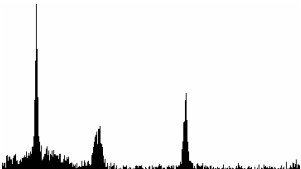
	Input pattern	Structural places	Histograms of the phase of orientations
Rotation -22°			
Rotation 0°			
Rotation $+22^\circ$			

Fig. 4. Comparison of rotated versions of a sign and their phase histograms. Rotation of a sign denotes horizontal modulo-shift of its phase histogram (each containing 360 bins).

Let us assume that we have two histograms, represented as vectors \mathbf{a} and \mathbf{b} , each consisting of N data, i.e. $\mathbf{a}=\{a_i\}_{1 \leq i \leq N}$ and $\mathbf{b}=\{b_i\}_{1 \leq i \leq N}$. The two probabilities associated with \mathbf{a} and \mathbf{b} can be approximated respectively as follows:

$$P(a_i) \approx a_i / \sum_{k=1}^N a_k = a_i / A, \text{ and } P(b_i) \approx b_i / \sum_{k=1}^N b_k = b_i / B. \quad (19)$$

The first tested was the Minkowsky measure which takes on the following form:

$$D_{M,r}(\mathbf{a}, \mathbf{b}) = \left[\sum_{i=1}^N |P(a_i) - P(b_i)|^r \right]^{\frac{1}{r}}. \quad (20)$$

Further, the Kullback measure D_K was tested, which is defined as follows [3]:

$$D_K(\mathbf{a}, \mathbf{b}) = \sum_{i=1}^N P(a_i) \log \frac{P(a_i)}{P(b_i)} = \log \frac{B}{A} + \frac{1}{A} \sum_{i=1}^N a_i \log \frac{a_i}{b_i} \quad (21)$$

where A and B are defined in (19). It is also assumed that for all i : $P(a_i) \neq 0, P(b_i) \neq 0$.

The other distance that was tested in our experiments is based on an approximation of the χ^2 distribution. It is given as follows:

$$D_{\chi^2}(\mathbf{a}, \mathbf{b}) = \sum_{i=1}^N \frac{[P(a_i) - P(b_i)]^2}{P(a_i) + P(b_i)}, \text{ assuming } P(a_i) + P(b_i) \neq 0. \quad (22)$$

D_{χ^2} has a nice feature of boosting response (i.e. lowering value of D_{χ^2} , in effect) obtained for relatively larger values of $P(a_i)$ and $P(b_i)$. This is very desirable since, intuitively, larger probabilities convey more important information.

However, during experiments we noticed a necessity to support highly probable phase orientation with simultaneous suppression of improbable values, which are mostly due to noise and some local orientation with minimal support. For this purpose we propose a modification of (22) in which the denominator is also squared

$$D_H(\mathbf{a}, \mathbf{b}) = \sum_{i=1}^N \left[\frac{P(a_i) - P(b_i)}{P(a_i) + P(b_i)} \right]^2, \text{ for all } P(a_i) + P(b_i) \neq 0. \quad (23)$$

Due to its properties D_H was used in the presented experiments.

5 Experimental Results

The code was written in C++ in Microsoft Visual 6.0. Experiments were performed on the IBM PC with Pentium IV 3.4GHz, 2GB RAM. The two data bases were used: The patterns in the first DB, depicted in Fig. 7a, were cropped from the real scene examples. The second DB was created from a drawings in a formal specification of TSs [17]. These are depicted in Fig. 7b.

Fig. 5 presents experimental results of detection and classification of two road signs in a real image. Shapes detected by the window growing technique are visible in Fig. 5b; Areas of the stick tensor of the pictograms are visualized in Fig. 5c,d.

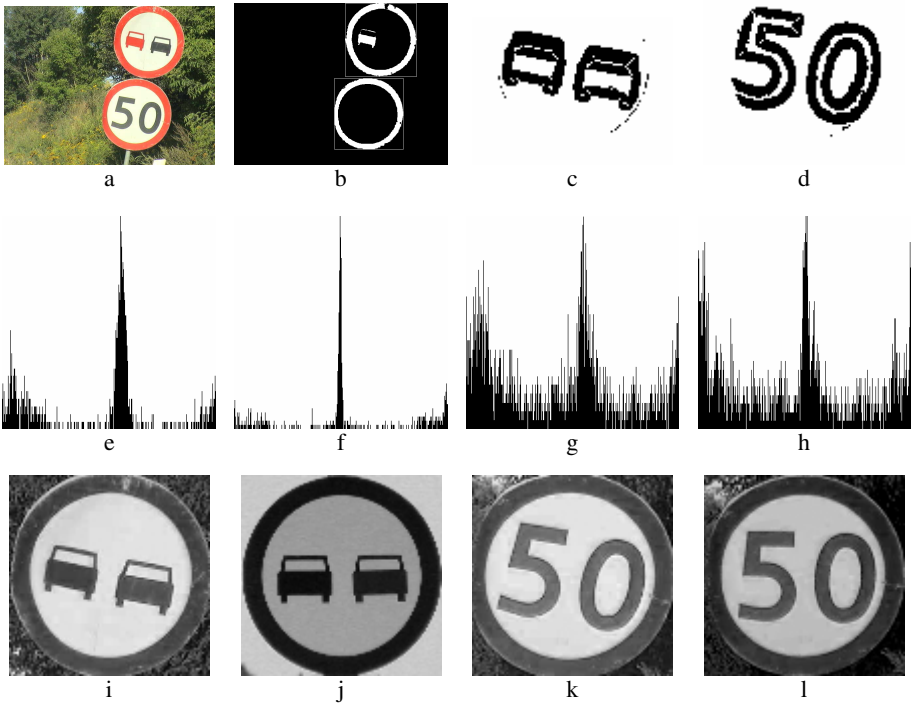


Fig. 5. Experimental results of detection and classification of the two road signs in an image (a). Detected shapes by the window growing technique (b). Areas of the stick tensor of the pictograms (c,d). Matched histograms of the top sign (e,f) and bottom sign (g,h). An observed sign and a corresponding sign found in the data-base (from real examples) (i,j) and (k,l).

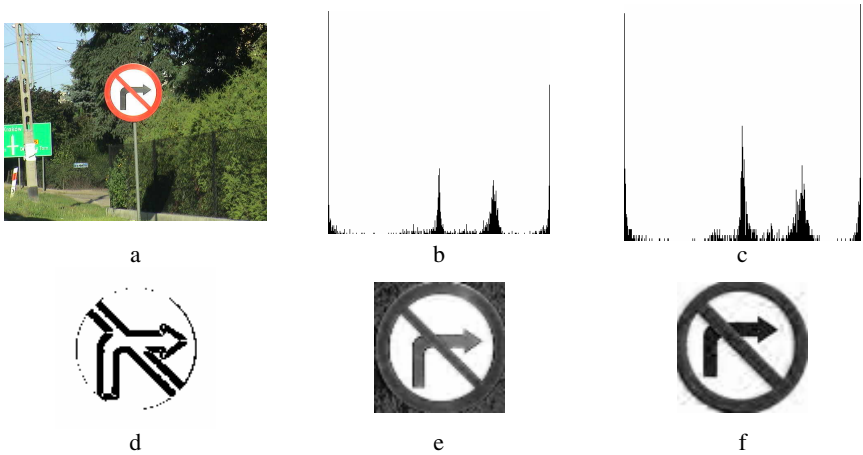


Fig. 6. Recognition results of a prohibition sign “No right turn” (a). Histograms of the test sign and a corresponding sign in a data base (b,c). A map of the stick tensor (d). Test pattern from the input image (e), and system response from the data base (f) – let’s notice the differences.

Matched histograms of the top sign are presented in Fig. 5e,f, and of the bottom sign in Fig. 5g,h. The sign of a scene and a sign found in the data base (containing prototypes from real examples) are in Fig. 5i,j and in Fig. 5k,l, respectively.

Fig. 6 depicts results of recognition of a prohibition sign “No right turn”. Histograms of the test sign and a corresponding sign in the data base are in Fig. 6b,c. A map of the stick tensor in Fig. 6d. Test pattern from the input image are shown in Fig. 6e, and system response from the data base in Fig. 6f.

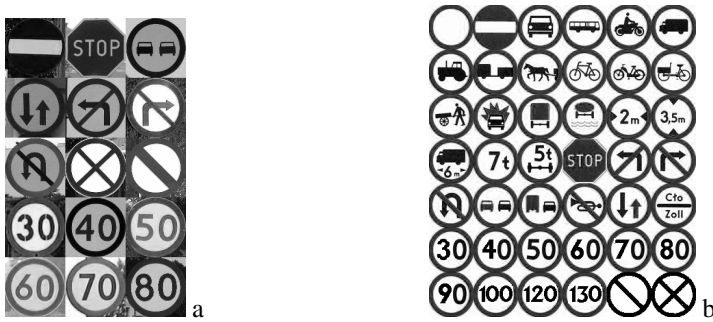


Fig. 7. Two data bases used in our experiments. The DB from (a) is constructed from prototypes cropped from real traffic scenes. The DB in (b) is created from the formal specification of the road signs, given in [17].

Parameters of the detector with adaptive window are discussed in [4]. Here we report only results of the recognition with the phase histograms. Two groups of circular signs were used: the prohibition signs (group “B”) and obligation signs (“C”). Quality is measured with the rate of true positives, which are presented in Table 1. The tests were obtained from approximately two hundreds of real traffic scenes.

It is interesting to compare quality of the proposed method with the similar method of orientation histograms which is based on simple edge detection [13][10]. Additionally we tested a modified edge-based method in which edges were morphologically dilated to increase their support in histograms. The comparison shows better results of the proposed method operating in the tensor field (Table 1).

Table 1. Accuracy of recognition (rate of true positives) for different methods and two groups of signs, prohibition “B”, and obligation “C”, at daily conditions

Method/Group	Prohibition signs	Obligation signs
ST based (this paper)	0.88	0.91
Dilated Edge	0.84	0.85
Edge	0.73	0.70

As alluded to previously, the proposed method incorporates some kind of edge detection (step 4 in the algorithm). However, it is an average gradient which is less prone to noise. The main difference then is that classification is done on phases of the stick components of the ST rather than on phases of noisy edges.

The obtained results show relatively high precision of the system. Nevertheless the systems that utilize neural committee machines operating with deformable models shows better quality [4][5]. However, the presented system operates faster (up to 10 frames per second) and requires much less memory, especially for circular signs. The group of obligation signs is smaller than the group of prohibition signs and therefore the classification parameters are slightly better for the former (see Table 1).

6 Conclusions

The presented method for traffic signs recognition is very fast and accurate. It is also highly tolerant to the small occlusions, translations, rotations, and symmetrical change of scale. This feature is very important due to imprecision of the detection module. When matching phase histograms it is important to gather statistically sufficient evidence of features. This means that the prototype images, as well as the matched ones, have to be large enough. This does not affect much the computation time, since the number of bins in the histograms is set separately. In our experiments we noticed that size of the matched images should be no less than 100×100 pixels for reliable matching. Number of the histogram bins controls resolution of the acquired orientation levels. This should not exceed the precision of the ST phase detector. Our experiments show that a sufficient number of bins is in the range of 180-360, i.e. the resolution from $2\text{-}1^\circ$. The method works fine with different lighting conditions such as day, night or rain conditions. Small occlusions are also tolerable, especially if they do not occlude significant area of a pictogram. The other main conclusions are summarized below:

1. It is *not* necessary to register test images. However, a slightly better results are obtained if they are registered.
2. The method is more precise than orientation histograms from edge detectors (However, it was compared only for the TSs classification problem).
3. Invariance to translation, rotation, and scale is necessary due to inaccuracy of the detection module (here the window growing technique is proposed for detection).
4. The method is not as precise as the deformable models. However, it requires much less memory and is faster (especially for rotation).
5. Four histogram matching measures were tested. The proposed new chi-square-square-based measure (23) performs the best. This is caused by promotion of the matches of the more numerous bins, i.e. the more probable features. To cope with potential rotations of the signs, the modulo shifted matching method was implemented. This means that modulo shifted versions of the prototype histograms are compared, and the best one is reported as a winner. Thus, as a side product we obtain a value of rotation of the recognized sign.
6. One threshold value is necessary. However, it is not very sensitive.
7. Sufficient number of bins should be in the range of 180-360.
8. Good results are obtained with the Farid 3×3 tap filters [9]. For these, hardware implementation is relatively cheap.
9. Good results are obtained for images of size 100×100 or higher. In such images the evidence is statistically sufficient for reliable classification. This can be obtained from smaller images in the registration process by affine scaling. Two data-bases were tested: one, created from the formal specification of the TS, the second, created from the ten examples of real signs.

10. The simplicity of the classification stage has a great influence on the total response time of the system (i.e. detection *and* classification), which is in the order of 90 ms per sign (resolution: 320×240). This is a very good result especially when compared with other similar systems [5].

Nevertheless, the method is not free from some problems. It requires setting of a threshold value for the structural places. Although, these is not a very sensitive parameter, it influences a quality of recognition – if not correctly set, then not all important areas can be taken for classification.

Acknowledgements

This work was supported from the Polish funds for the scientific research in 2008.

References

1. Bigün, J., Granlund, G.H., Wiklund, J.: Multidimensional Orientation Estimation with Applications to Texture Analysis and Optical Flow. *IEEE PAMI* 13(8), 775–790 (1991)
2. Brox, T., Boomgaard van den, R., Lauze, F., Weijer van de, J., Weickert, J., Mrázek, P., Kornprobst, P.: *Adaptive Structure Tensors and their Applications*, pp. 17–47. Springer, Heidelberg (2006)
3. Cover, T.M., Thomas, J.A.: *Elements of Information Theory*, 2nd edn. Wiley, Chichester (2006)
4. Cyganek, B.: Circular Road Signs Recognition with Soft Classifiers. *Integrated Computer-Aided Engineering* 14(4), 323–343 (2007)
5. Cyganek, B.: Rotation Invariant Recognition of Road Signs with Ensemble of 1-NN Neural Classifiers. In: Kollias, S.D., Stafylopatis, A., Duch, W., Oja, E. (eds.) *ICANN 2006*. LNCS, vol. 4132, pp. 558–567. Springer, Heidelberg (2006)
6. Cyganek, B.: Real-Time Detection of the Triangular and Rectangular Shape Road Signs. In: Blanc-Talon, J., Philips, W., Popescu, D., Scheunders, P. (eds.) *ACIVS 2007*. LNCS, vol. 4678, pp. 744–755. Springer, Heidelberg (2007)
7. DaimlerChrysler, *The Thinking Vehicle* (2002), <http://www.daimlerchrysler.com>
8. Escalera, A., Armingol, J.A.: Visual Sign Information Extraction and Identification by Deformable Models. *IEEE Tr. On Int. Transportation Systems* 5(2), 57–68 (2004)
9. Farid, H., Simoncelli, E.P.: Differentiation of Discrete Multidimensional Signals. *IEEE Transactions on Image Processing* 13(4), 496–508 (2004)
10. Freeman, W.T., Roth, M.: Orientation Histograms for Hand Gesture Recognition, Mitsubishi Electric Research Laboratories, TR-94-03a (1994)
11. Gao, X.W., Podladchikova, L., Shaposhnikov, D., Hong, K., Shevtsova, N.: Recognition of traffic signs based on their colour and shape features extracted using human vision models. *Journal of Visual Communication & Image Representation* (2005)
12. Jähne, B.: *Digital Image Processing*, 4th edn. Springer, Heidelberg (1997)
13. McConnell, R.: Method of and apparatus for patt. recogn. US. Patent No. 4, 567, 610 (1986)
14. Mordohai, P., Medioni, G.: *Tensor Voting. A Perceptual Organization Approach to Computer Vision and Machine Learning*. Morgan & Claypool Publishers (2007)
15. Paclik, P., Novovicova, J., Pudil, P., Somol, P.: Road sign classification using Laplace kernel classifier. *Pattern Recognition Letters* 21, 1165–1173 (2000)
16. Pratt, W.K.: *Digital Image Processing*, vol. 3. Wiley, Chichester (2001)
17. Road Signs and Signalization. Directive of the Polish Ministry of Infrastructure, Internal Affairs and Administration (Dz. U. Nr 170, poz. 1393) (2002)